Received 5 January 2023; revised 4 February 2023; accepted 10 February 2023. Date of publication 24 February 2023; date of current version 9 March 2023.

Digital Object Identifier 10.1109/OJAP.2023.3248610

Series-Fed Millimeter-Wave Antenna Array Based on Microstrip Line Structure

SUMIN DAVID JOSEPH AND EDWARD A. BALL (Member, IEEE)

Department of Electronic and Electrical Engineering, The University of Sheffield, S10 2TN Sheffield, U.K.

CORRESPONDING AUTHOR: S. DAVID JOSEPH (e-mail: s.d.joseph@sheffield.ac.uk)

This work was supported by the U.K. Research and Innovation (UKRI) Future Leaders Fellowship under Grant MR/T043164/1.

ABSTRACT This paper presents a millimeter wave series-fed microstrip line antenna array with low side lobes. For millimeter-wave beam forming applications, compact series fed arrays with very small horizontal width and low side lobes are very much required. The proposed array consists of a microstrip line with periodically placed stepped inverted-cone stub sections at a guided wavelength spacing. Surface current cancellation at each guided wavelength in an ideal microstrip line can be altered by symmetrically introducing the inverted-cone stub sections on two edges with a half wavelength offset. By controlling the dimensions and location of the inverted-cone stub sections, the equivalent surface currents can be altered and focused on the cone stub sections, resulting in an effective array radiation. The fabricated antenna array is resonating at 28 GHz and has an impedance bandwidth of 1.3 GHz. Peak realized gain of 10.2 dBi is achieved at 28 GHz and the measured side lobe levels are better than −15 dB in the E and H plane. The proposed microstrip line antenna array with low side lobes also benefits from simple fabrication and high integration ability, which makes it attractive for compact beamforming scenarios in millimeter-wave bands.

INDEX TERMS Antennas, antenna array, low sidelobe level (SLL), millimeter-wave (mm-wave) array, series-fed array, transmission lines.

I. INTRODUCTION

THE RAPID increase in the data traffic of wireless networks due to the dramatic surge in wireless communication systems challenges the available spectrum resources [1]. Millimeter-wave (mm-wave) frequency bands have been receiving higher attention over the recent years as they have been demonstrated to meet the requirements of high data rate and large capacity [2]. Thus, several mm-wave frequency bands for the fifth-generation (5G) communications have been approved by the International Telecommunication Union (ITU), including 24.25–27.5, 37–40, and 66–76 GHz [3]. Therefore, a sudden surge in the investigation of efficient compact high frequency antennas is emerging [4].

Due to the low fabrication cost, low mass, and small profile, microstrip antenna arrays have been extensively used in mm-wave systems compared to waveguide antennas [5]. However, microstrip arrays suffer from quite high losses compared to waveguide designs [6]. Losses are mainly due to dielectric and conductor losses, which are directly related to the total antenna length [7]. Therefore, great care is essential to choose the required feeding technique. Series and parallel feeding are usually used in microstrip arrays. As the feed of each element in a parallel array can be adjusted by the carefully designed feeding network, it is straightforward to attain high gain, broad bandwidth [8], [9], and minimum sidelobe level (SLL) [10]. Nevertheless, the complicated larger feeding length led to high losses and bulky size. In contrast, the series-fed array has a compact arrangement and simple feed structure [11].

To decrease the susceptibility to interference and thus increase the received signal quality, low side lobe level is required along with high directivity in an array antenna for wireless communication and sensor applications [12]. To attain a low SLL and to shape the radiation pattern, substantial investigation has been conducted on microstrip arrays with series feed structure [13], [14]. A general technique for making varying excitation is to adjust the efficiency by

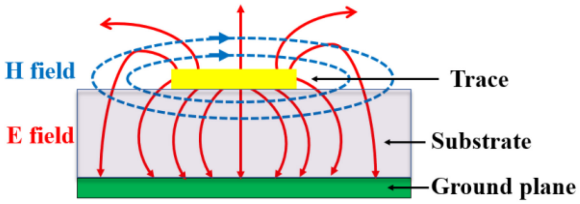

FIGURE 1. Electric field (E) and magnetic field (H) distribution in the cross-section of a microstrip transmission line.

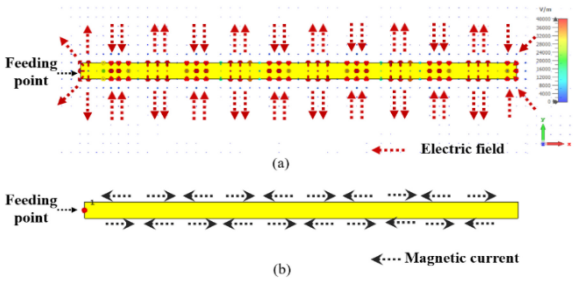

FIGURE 2. (a) Simulated electric field distribution and (b) corresponding magnetic current along the length of an ideal microstrip transmission line.

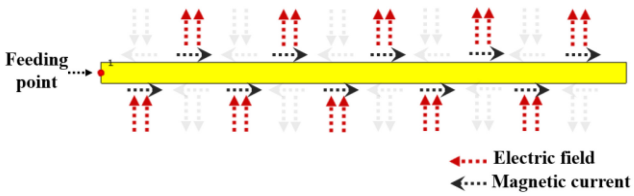

FIGURE 3. Proposed electric field distribution and the corresponding magnetic current along the length of a microstrip transmission line for effective radiation.

altering the width of the patch of each antenna element [15]. In this, moderately larger power is distributed in the centre of the array and a lesser power is distributed towards both ends of the array. This typically means adjusting the array amplitude using polynomial coefficients such as Binomial, Chebyshev, and Taylor series [16], [17], [18]. Meanwhile the radiations from individual elements are different, so this technique affects the overall gain and is useful only with small amplitude tapering. Or else, the generated beam profile would be severely affected.

In this work, a novel microstrip line antenna array is studied. A preliminary design of the proposed antenna with comparably low bandwidth was mentioned in [19]. In this article, we present the simulation results and lab measurements of an improved design and provide design guidelines. This paper is organized as follows: Section II discusses the general working principle of the microstrip line array. Section III presents the design and mechanism of the proposed series-fed line array; design strategy and parametric analysis is also carried out in this section. Section IV discusses the performance of the microstrip line array with measurement results. Finally, Section V presents the conclusions.

II. RADIATION MECHANISM OF MICROSTRIP ARRAY

In RF circuits, the microstrip transmission line is widely recognized due to its effectiveness in integrating microwave devices and simple fabrication processes. As it is a waveguiding structure, the radiative property of an ideal microstrip line is intentionally limited due to its unique field distribution. The dominant mode of a microstrip line is a quasi-TEM mode. Specifically, the electric field is mostly contained in the dielectric but also fringes up above the dielectric into the free space as in Fig. 1. Fig. 1 shows the cross-section of a microstrip transmission line.

To investigate the field and current distributions, a microstrip line is analyzed with a 50 Ω feed at one end as shown in Fig. 2. In every half wavelength, the fringing electric field reverses its direction, and it shows a periodic waveform along the microstrip line. Subsequently, the equivalent magnetic currents are parallel to the edges of the microstrip line. Moreover, the magnetic current along both sides of the microstrip line have the same amplitudes but are in antiphase. Therefore, the radiated fields cancel out on both edges of the line. This property is very beneficial to diminish the crosstalk between adjacent microstrip lines and to decrease the radiation losses when the microstrip line is used as a guiding transmission line structure.

For making the transmission line radiative, it is required to cancel the magnetic currents alternatively from both edges of the microstrip line, as shown in Fig. 3. The proposed novel series-fed array with microstrip line feeding is aimed to use for millimeter wave applications especially for integrating with MMIC and other integrated circuits due to its compact horizontal width and low side lobes. Most of the other microstrip line-based antenna arrays [20], [22] has vertical blocking metallic plates and shorting pins for removing the surface current cancellation in an ideal microstrip line. Moreover, these vertical metallic plates and shorting pins are difficult to fabricate in millimeter wave frequencies due to the small dimensions. Therefore, our major contribution of this work is to develop a compact planar series fed array without using any complex structures like vertical metallic plates and shorting pins. In this design, the inverted-cone stub sections are introduced on the two sides of the transmission line to change the properties of a simple transmission line. The inverted cone stub sections alter the electric field distribution to one direction as opposed to the periodic opposite phases of an ideal microstrip line. Correspondingly, the stepped inverted cone stub sections aid to eliminate the cancelling surface currents and to make the transmission line radiative. Compared to other reported microstrip line arrays, the proposed array doesn't have any shorting pins at the ends of the microstrip line. Thus, the feeding is achieved easily by connecting a 50-ohm microstrip line to the end of the transmission line. Therefore, the proposed array can be directly integrated to the mm wave and MMIC circuits. Comb line and other stub based radiating elements have been widely used in series fed antenna arrays for reducing the losses by minimizing the total pattern length. Even though it slightly

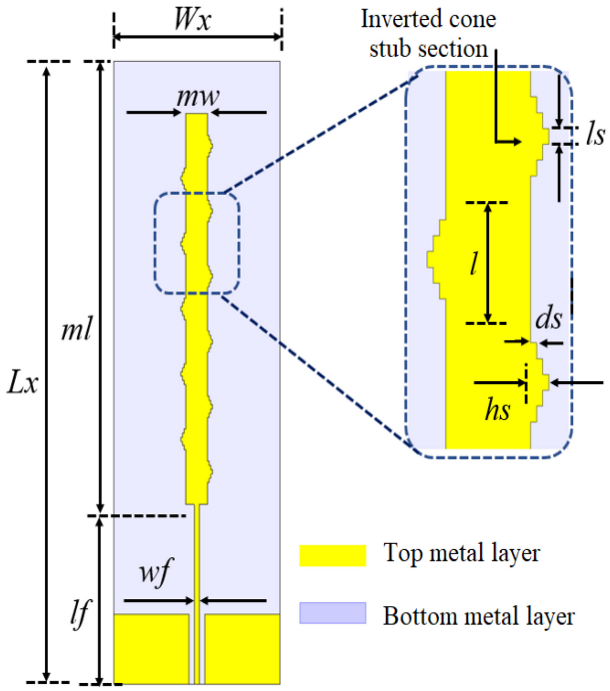

FIGURE 4. Geometry of the proposed array antenna. Inset shows the enlarged image of the stubbed inverted cone stub sections.

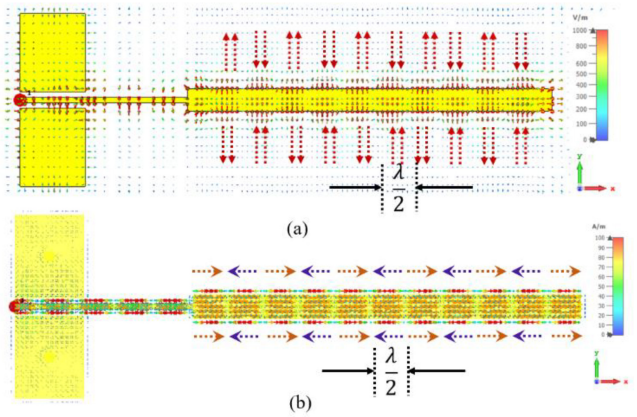

FIGURE 5. (a) Simulated electric field distribution and (b) corresponding surface current at 28 GHz along the microstrip transmission line without the stepped inverted-cone stub sections.

reduces the antenna area, the design complexity for such existing approaches is significantly high and difficult [26]. Thus, the proposed new, simple to use, design concept in this article is beneficial for compact beamforming scenarios in mm-wave bands.

III. MICROSTRIP LINE BASED SERIES-FED ANTENNA ARRAY

In this section, a microstrip line-based series-fed array at 28 GHz is proposed and studied to evaluate the aforementioned radiation mechanism as depicted in Fig. 3. Fig. 4 shows the geometry of the proposed array. A microstrip line with a length *ml* of 6λ and a width *mw* of 0.36λ is designed as the main radiating element. For achieving the effective radiation, stepped inverted-cone stub sections are introduced on both edges of the microstrip line. The stepped inverted cone stub sections aid to eliminate the cancelling surface currents and to make the transmission line radiative. A resultant current distribution in the stub's direction is realized by placing the inverted cone stub sections in every wavelength in the two sides symmetrically with an offset. Five stub strips are comprised in each stepped inverted-cone stub section. The height of stub strips in each section increases to a maximum value *hs* of 0.45 mm and then decreases. Each strip has a constant stub length *ls* of 0.35 mm. Rogers RO4003C substrate with a thickness of 0.2 mm is utilized for the proposed antenna and it has a total size of 50 × 15 mm. The substrate has a permittivity ε_r of 3.55 and loss tangent of 0.0027.

In order to support a direct integration into mm-wave and MMIC circuits, a 0.45 mm thick 50 ohm microstrip line is connected to the end of the line array. A long microstrip feed line is used to avoid any parasitic coupling effects from the connector while performing the pattern measurements. A rectangular ground plane is positioned on the back side of the substrate.

To illustrate the mechanism of the proposed series-fed array, primarily a simple microstrip line without the stepped inverted cone stub sections is examined. Fig. 5 illustrates the electric field distribution and surface current in the conventional microstrip line. It can be seen that the fringing electric field has similar amplitudes but opposite phases along the edges of the microstrip line. Also, it is symmetric and periodic along the length of the line. Subsequently, the equivalent surface currents along the microstrip line reverse direction in each half wavelength as shown in Fig. 5(b). Thus, cancellation of the resultant surface current occurs in every guided wavelength [21], [22]. Therefore, conventional microstrip line cannot be used for radiation, as is well known.

Now, stepped inverted-cone stub sections are symmetrically introduced on both edges of the microstrip line with an offset of a half wavelength as shown in Fig. 4. To remove the cancelling of surface current, five stub strips with a combined length of not more than λ/2 are utilized in each section. It can be observed from Fig. 6(b) that the resultant surface currents are now directed to the stepped inverted-cone sections of the microstrip line. Moreover, the resultant electric field distribution in Fig. 6(a) is now focused in one direction as opposed to the periodic opposite phases of an ideal microstrip line. A high gain array with low SLL can be easily realized by appropriately altering the dimensions of the inverted-cone stub sections.

Stepped inverted cone stub sections have significant effects on perturbing the field distribution and the antenna performance. In a parametric study, only one parameter is varied at a time and the others are kept invariant. The dimensions and the location of the stepped inverted cone stub section have great influence on operating frequency and impedance matching. The influence of the microstrip line and

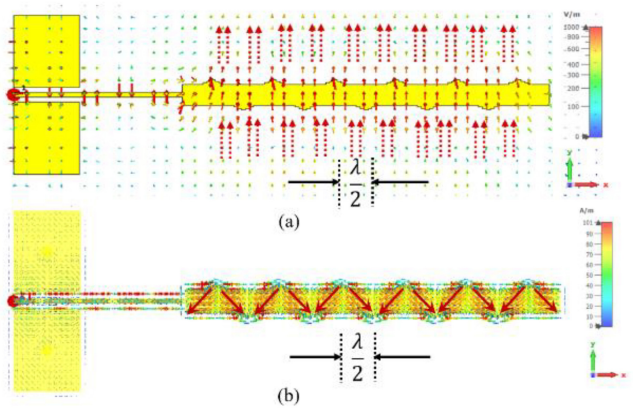

FIGURE 6. (a) Simulated electric field distribution and (b) corresponding surface current at 28 GHz along the proposed microstrip line antenna.

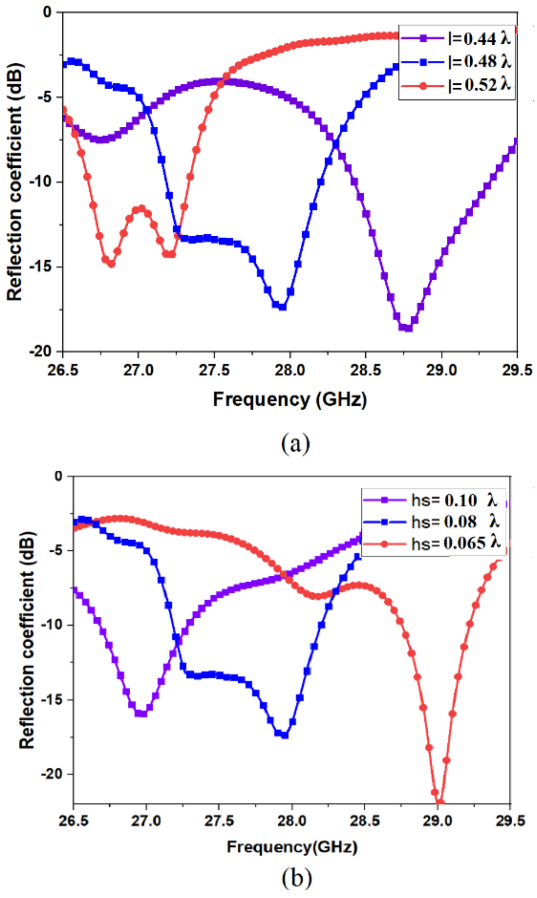

FIGURE 7. Simulated reflection coefficients of the proposed microstrip line array for different (a) microstrip-line lengths *l* and (b) inverted cone stub height hs.

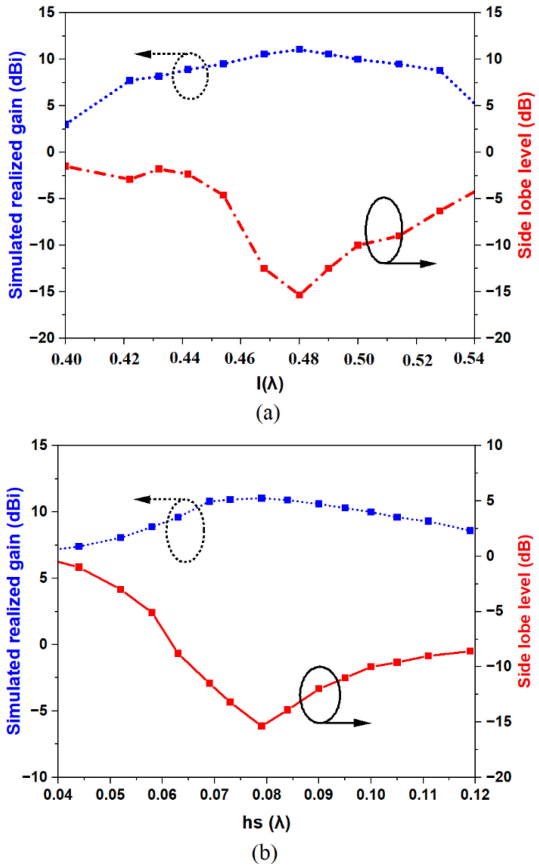

FIGURE 8. Simulated realized gain and side lobe levels of the microstrip array with (a) microstrip-line lengths *l* and (b) stepped inverted cone stub height hs.

the location of the stepped inverted cone stub is studied and shown in Fig. 7(a). It can be seen that the resonant frequency shift downward from 28.8 to 27 GHz when l increase from 0.44 to 0.52λ, as might be intuitively anticipated.

Fig. 7(b) depicts the change in resonant frequency of the proposed antenna array for different stepped inverted cone stub height of $hs = 0.065$, 0.08, and 0.1λ. It can be clearly observed that the resonance shifts downward significantly with increasing hs. To be more specific, when hs increases from 0.065 to 0.1λ, the resonant frequency moves from 29 to 27 GHz, demonstrating that the inverted cone stub height can be utilized to tune the operating frequency of the array.

To investigate the proposed microstrip line antenna array at 28 GHz, the microstrip line antenna dimensions is varied to analyze the realized gain and side lobe levels performance as shown in Fig. 8. The relationship between realized gain and side lobe levels with microstrip line length l is shown in Fig. 8(a). It can be seen that the realized gain reaches a maximum of 11.05 dBi with a line length of nearly 0.48λ at 28 GHz. Moreover, the SLL are better than −15 dB at this line length. The change in realized gain is not a strong function of line length. However, the side lobe levels do vary rapidly with the line length. Similarly, an optimum height of inverted cone stub section can be deduced from the Fig. 8(b). The maximum gain and minimum side lobe levels are observed at a stub height of 0.08λ. Fig. 9 shows the impedance for different line widths. It can be seen that the impedance bandwidth has significant dependency on the width of the microstrip line. As the width of the line increases from 0.33 to 0.39λ, the impedance circle radius increases, degrading the match. The width of the microstrip line is optimized to 0.36λ to achieve a wide

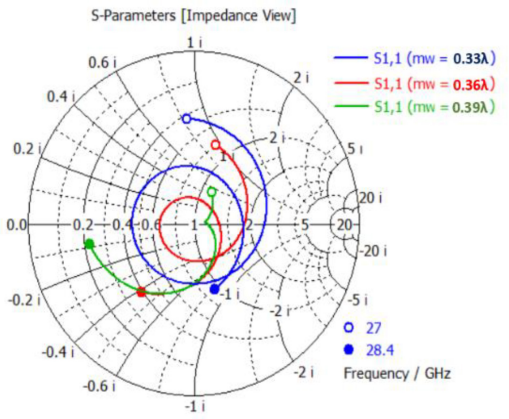

FIGURE 9. Smith chart showing the input impedance for different line widths.

−10 dB impedance bandwidth. Considering the relationship between the frequency and the discussed parameters, the following equation can be used to estimate the operating frequency:

$$f \approx \frac{c}{\sqrt{\epsilon_r} \times \sqrt{(\lambda)^2 + (mw + 3 \times ds)^2}} \quad (1)$$

where c is the velocity of light in vacuum, λ is the guided wavelength and ε_r represents the effective dielectric constant of microstrip line considering the dispersion effect. Based on the above analysis, and in order to design and analyse the proposed microstrip line antenna array, initially the length l can be used to estimate the length of the array. Each stepped inverted section requires a l length as in Fig. 4. For initiation, the microstrip line dimensions can be estimated as $l \approx \lambda/2$ and $mw \approx \lambda/3$. Then, initial dimensions of the stepped inverted cone stub sections can be initialized as $5ls \leq \lambda/2$ and $3ds \approx \lambda/12$. Then, insert the feeding line at the end of microstrip line. The resultant feeding impedance at the end of the array will be approximately 50 Ω. Finally, optimize the microstrip line and stepped inverted cone stub dimensions to realize the required operating frequency, return loss and radiation pattern. EM simulations were performed using CST studio.

Another promising advantage of the proposed antenna array is its scalability along the length direction. The directivity of the antenna increases with the length of the microstrip line antenna as shown in Fig. 10. Initially, an array with 2λ length (3 inverted cones) is analyzed and observed a directivity of around 8 dBi. Directivity increased to nearly 9.5 dBi with 3λ length (5 inverted cones). Likewise, the directivity is further increased to 12.5 dBi with an increased length of 6λ (11 inverted cones). Further minor length increases will only lead to a slight increase in directivity, due to the effective array factor due to the additional cones. The resulting directivity with respect to the 2λ case is seen to increase by approximately 10log(N/3). Overall, the fabrication is comparatively easy, as this design removes vertical blocking metallic plates and shorting pins compared to [20], [22].

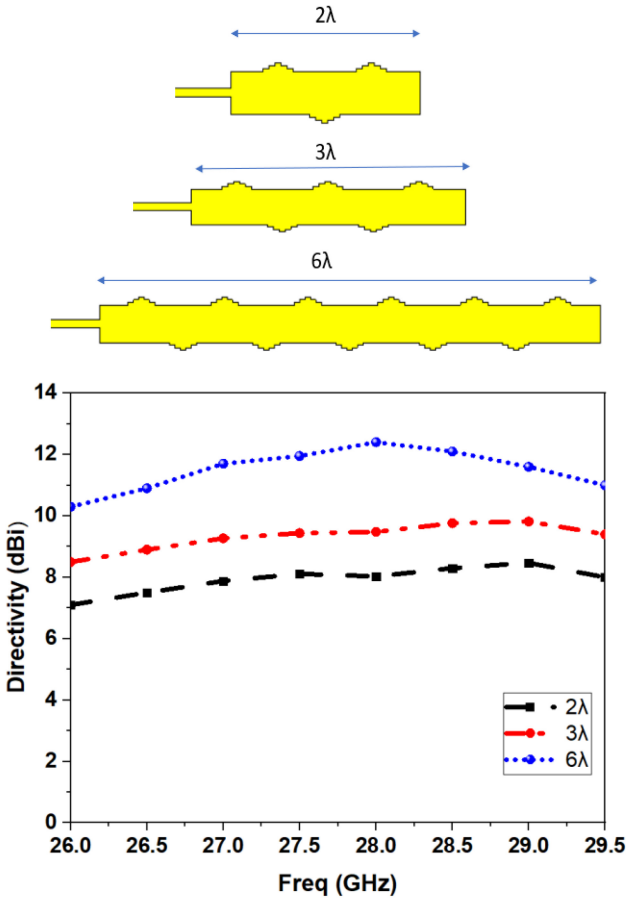

FIGURE 10. Boresight directivity of three different microstrip linear arrays with length 2λ, 3λ and 6λ.

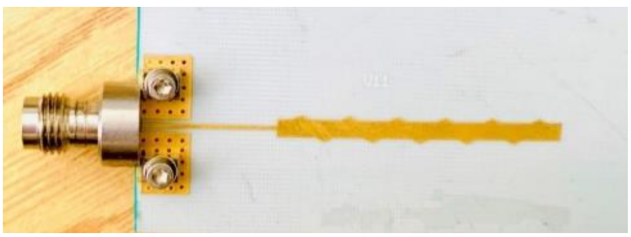

FIGURE 11. Fabricated microstrip line antenna array.

IV. PERFORMANCE OF THE MICROSTRIP LINE ARRAY

To validate the feasibility of the proposed design, a microstrip line antenna array is fabricated with a length of 6λ, as shown in Fig. 11. The antenna prototype is connected with a 2.4 mm edge launch connector ELF50. The impedance bandwidth is measured with an Agilent N5247A VNA. The simulated and measured impedance matching of the line array is shown in Fig. 12. Antenna array is resonating at 28 GHz as designed. The fabricated microstrip line antenna array has an impedance bandwidth of 1.3 GHz ranging from 27 to 28.3 GHz. The measured bandwidth is slightly wider than the simulated one. This disagreement is likely due to simulation or loss tangent errors.

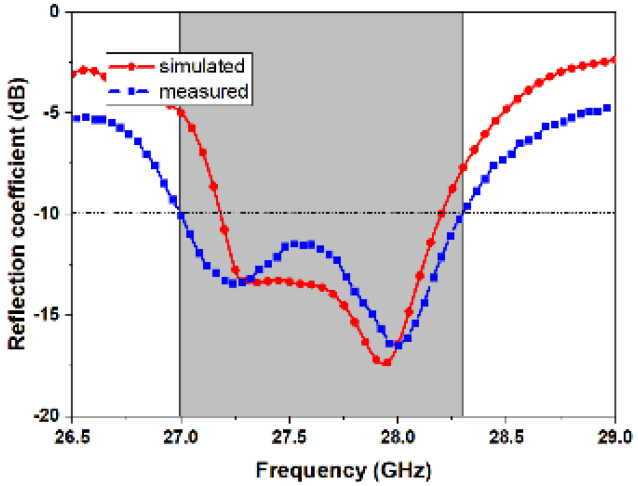

FIGURE 12. Simulated and measured reflection coefficients.

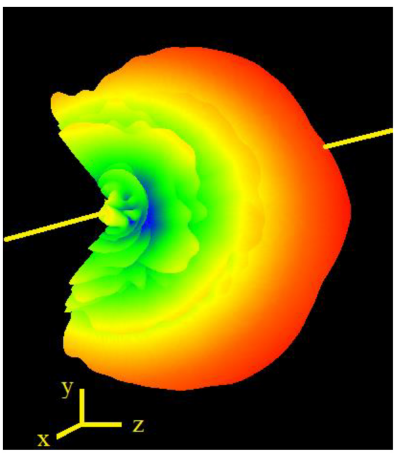

FIGURE 13. Measured 3-D radiation pattern of the microstrip line antenna array.

The beam profile and radiation performance of the fabricated array was evaluated using the NSI-MI 700S-360 system in TUoS mm-wave Lab [23]. Fig. 13 represents the measured three dimensional beam pattern of the fabricated array antenna. Antenna array is in the X-Y plane and the peak radiation is in Z direction as in Fig. 13.This microstrip line array has the main beam towards broadside direction. The realized gain and side lobe levels of the proposed array antenna are presented in Fig. 14. A maximum gain of 10.2 dBi is measured at 28 GHz, agreeing well with simulation. The simulated gain value ranges from 8.39 to 11.05 dBi across the impedance band and the peak value is 10.7 dBi at 28 GHz, while the measured gain ranges from 8.1 to 10.2 dBi. Minimum side lobe level of −16 dB is achieved at 27.6 GHz and side lobe levels are better than −15 dB in the range of 27.24 to 28.26 GHz.

Fig. 15 shows the simulated and measured co-polarized and cross polarized normalized radiation patterns of the array antenna at 28 and 27.5 GHz in the H plane. The measured values are in the angular range of 120° to −120° (240°). A narrow beam with a 3 dB beam width of about

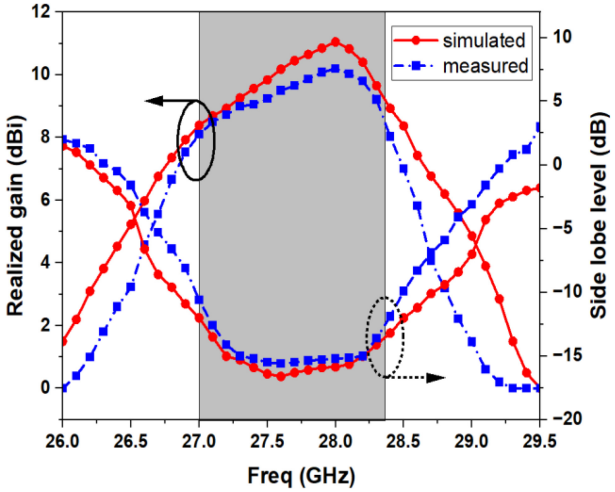

FIGURE 14. Realized gain and side lobe levels of the antenna array.

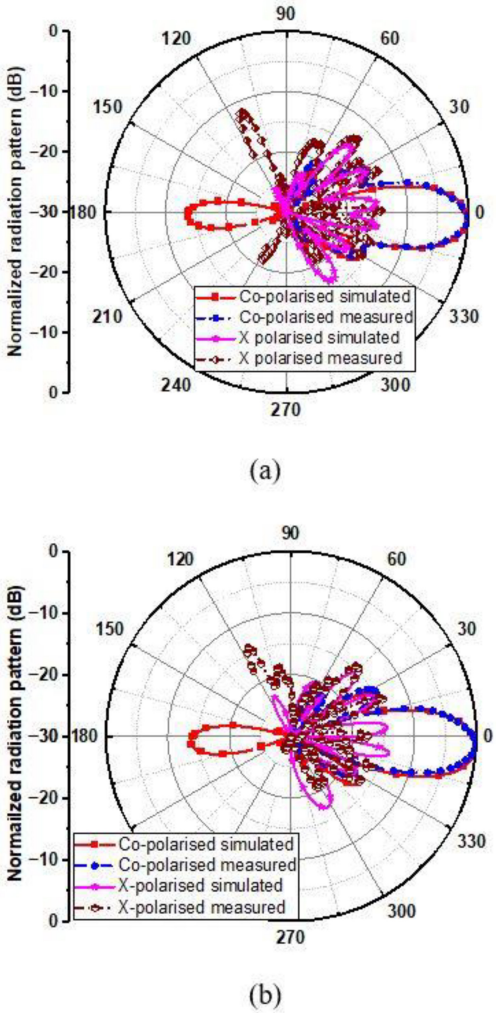

FIGURE 15. Simulated and measured normalized radiation pattern of the array in the H-plane (a) 28 GHz (b) 27.5 GHz.

16° and 17° is obtained in the H-plane (($\varphi = 0°$) at 28 and 27.5 GHz respectively. The radiation pattern of simulated and measured curves follows a similar form. Even

TABLE 1. Comparison of some recent series-fed arrays.

Reference	Description	Freq (GHz) &Bandwidth	Gain at center frequency (dBi)	Size (λ_0^2)	Complexity	SLL(dB)
[24]	Angled dipole uniform array	28 23.3-51	10.4	3.06 × 1	simple	-7
[25]	Inclined slot-fed uniform array	28 27.2-29.6	11.65	NA	complex	-10
[26]	Microstrip comb-line linear array antenna	28 23.5-33.1	15	8.65 × 1.8	complex	-23
[27]	Transverse Slot Array in Groove Gap Waveguide	28 27.6-28.6	NA	4.37 × 1.35	average	-11
[28]	Dolph-Chebyshev tapered patch Antenna Array	26 24.8-27.1	9	8.67 × 3.90	simple	-12
[29]	79 GHz Stacked Micro-Via Loading	79 74.5-85.8	12.67	6.06 × 0.57	complex	-12.9
This work	**Microstrip line uniform array**	**28 27-28.3**	**10.7**	**4.5 × 1.35**	**Simple**	**-15**

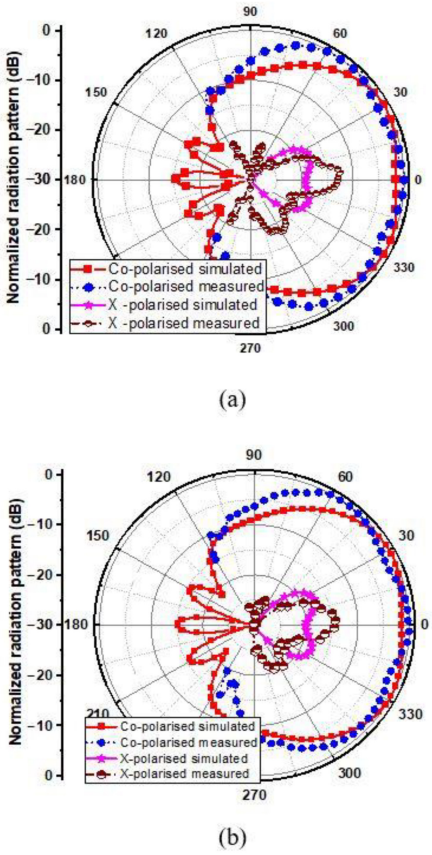

FIGURE 16. Simulated and measured normalized radiation pattern of the array in the E-plane (a) 28 GHz (b) 27.5 GHz.

though slight discrepancies are visible in the side lobes and minor lobes region, a good similarity can be observed in the main lobe pattern and beamwidth. Side lobe levels in the H-plane are better than −15 dB at 28 and 27.5 GHz. The simulated and measured co-polarized and cross polarized normalized radiation patterns of the array antenna in the E plane ($\varphi = 90°$) at 28 and 27.5 GHz is represented in Fig. 16. The E-plane pattern has a fan shape, and the 3 dB beam width of about 142° and 148° at 28 and 27.5 GHz respectively. Measured beamwidth is slightly wider than simulated at both the frequencies. Side lobe levels in the E-plane is also better than −15 dB at 28 and 27.5 GHz as shown in Fig. 16.

Finally, a comparison of the proposed design with other series-fed arrays is given in Table 1. Various kinds of series fed arrays are chosen for comparing the structural and conceptual differences. The proposed design offers a minimum SLL with good gain compared to [24], [25], [27], [28] and [29]. The antenna in [26] is a comb-line design with high gain and better SLL, but the size of the antenna is quite large, and the design procedure is complex compared to the proposed design. For using in compact beam steering scenarios, the proposed design is quite advantageous because of the very small width of the actual radiating microstrip line (0.27λ0). Even though the proposed microstrip line-based array has some conceptual similarity to the designs in [20], fabrication techniques, easy feeding, and low design complexity.

V. CONCLUSION

This paper presented a novel mm-wave series-fed microstrip line antenna array with low side lobes. Surface current cancellation in an ideal microstrip line was altered to make it an efficient radiator by introducing stepped inverted-cone stub sections on both edges of the microstrip line at one guide wavelength spacing. A microstrip line array having length of 6λ at 28 GHz has been fabricated and tested to demonstrate the concept. The proposed array achieved a 1.3 GHz impedance bandwidth, 8.1 to 10.2 dBi realized gain and a good broadside radiation pattern. A good side lobe level better than −15 dB has been achieved in the E and H-plane. A design strategy and key geometric relationships are identified and presented. The fabricated microstrip line antenna array has the advantages of wideband, low SLL

and high directivity. It also benefits from simple fabrication, low profile and high integration ability making it suitable for forthcoming communication standards.

REFERENCES

[1] J. Zhang, X. Ge, Q. Li, M. Guizani, and Y. Zhang, "5G millimeter-wave antenna array: Design and challenges," *IEEE Wireless Commun.*, vol. 24, no. 2, pp. 106–112, Apr. 2017.

[2] N. Garcia, H. Wymeersch, E. G. Ström, and D. Slock, "Location-aided mm-wave channel estimation for vehicular communication," in *Proc. IEEE Workshop Signal Process. Adv. Wireless Commun.*, Edinburgh, U.K., Jul. 2016, pp. 1–5.

[3] T. S. Rappaport et al., "Millimeter wave mobile communications for 5G cellular: It will work!" *IEEE Access*, vol. 1, pp. 335–349, 2013.

[4] M. J. Marcus, "5G and 'IMT for 2020 and beyond' [spectrum policy and regulatory issues]," *IEEE Wireless Commun.*, vol. 22, no. 4, pp. 2–3, Aug. 2015.

[5] Y. Al-Alem and A. A. Kishk, "Efficient millimeter-wave antenna based on the exploitation of microstrip line discontinuity radiation," *IEEE Trans. Antennas Propag.*, vol. 66, no. 6, pp. 2844–2852, Jun. 2018.

[6] S. Ghosh and D. Sen, "An inclusive survey on array antenna design for millimeter-wave communications," *IEEE Access*, vol. 7, pp. 83137–83161, 2019.

[7] A. Pandey, *Practical Microstrip and Printed Antenna Design*. Norwood, MA, USA: Artech House, 2019, pp. 322–324.

[8] H. Xu, J. Zhou, K. Zhou, Q. Wu, Z. Yu, and W. Hong, "Planar wideband circularly polarized cavity-backed stacked patch antenna array for millimeter-wave applications," *IEEE Trans. Antennas Propag.*, vol. 66, no. 10, pp. 5170–5179, Oct. 2018.

[9] B. Biglarbegian, M. Fakharzadeh, D. Busuioc, M.-R. Nezhad-Ahmadi, and S. Safavi-Naeini, "Optimized microstrip antenna arrays for emerging millimeter-wave wireless applications," *IEEE Trans. Antennas Propag.*, vol. 59, no. 5, pp. 1742–1747, May 2011.

[10] P. A. Dzagbletey and Y.-B. Jung, "Stacked microstrip linear array for millimeter-wave 5G baseband communication," *IEEE Antennas Wireless Propag. Lett.*, vol. 17, pp. 780–783, 2018.

[11] R. Chopra and G. Kumar, "Series- and corner-fed planar microstrip antenna arrays," *IEEE Trans. Antennas Propag.*, vol. 67, no. 9, pp. 5982–5990, Sep. 2019.

[12] R. Bayderkhani and H. R. Hassani, "Wideband and low sidelobe slot antenna fed by series-fed printed array," *IEEE Trans. Antennas Propag.*, vol. 58, no. 12, pp. 3898–3904, Dec. 2010.

[13] J. Yin, Q. Wu, C. Yu, H. Wang, and W. Hong, "Low-sidelobe-level series-fed microstrip antenna array of unequal interelement spacing," *IEEE Antennas Wireless Propag. Lett.*, vol. 16, pp. 1695–1698, 2017.

[14] H. Khalili, K. Mohammadpour-Aghdam, S. Alamdar, and M. Mohammad-Taheri, "Low-cost series-fed microstrip antenna arrays with extremely low sidelobe levels," *IEEE Trans. Antennas Propag.*, vol. 66, no. 9, pp. 4606–4612, Sep. 2018.

[15] B. Li, Y. Qiu, J. Zhang, Z. Zhou, and L. Sun, "W-band series-fed microstrip patch array with optimization of tapering profile," in *Proc. 9th Asia–Pacific Conf. Antennas Propag. (APCAP)*, 2020, pp. 1–2.

[16] J. C. Dash, D. Sarkar, and Y. Antar, "Design of series-fed patch array with modified binomial coefficients for MIMO radar application," in *Proc. IEEE Int. Symp. Antennas Propag. USNC-URSI Radio Sci. Meeting (APS/URSI)*, 2021, pp. 1027–1028.

[17] R. Chopra and G. Kumar, "Series-fed binomial microstrip arrays for extremely low sidelobe level," *IEEE Trans. Antennas Propag.*, vol. 67, no. 6, pp. 4275–4279, Jun. 2019.

[18] T. Yuan, N. Yuan, and L.-W. Li, "A novel series-fed taper antenna array design," *IEEE Antennas Wireless Propag. Lett.*, vol. 7, pp. 362–365, 2008.

[19] S. D. Joseph and E. A. Ball, "A novel millimeter-wave series-fed microstrip line antenna array," in *Proc. 16th Eur. Conf. Antennas Propag. (EuCAP)*, Madrid, Spain, 2022, pp. 1–4.

[20] L. Chang, Z. Zhang, Y. Li, and Z. Feng, "Wideband triangular-cavity-cascaded antennas," *IEEE Trans. Antennas Propag.*, vol. 64, no. 7, pp. 2840–2847, Jul. 2016.

[21] C. A. Balanis, *Antenna Theory: Analysis and Design*. Hoboken, NJ, USA: Wiley, 2016.

[22] L. Chang, Z. Zhang, Y. Li, and Z. Feng, "All-metal antenna array based on microstrip line structure," *IEEE Trans. Antennas Propag.*, vol. 64, no. 1, pp. 351–355, Jan. 2016.

[23] "University of Sheffield EPSRC mm wave measurement laboratory Website." Accessed: Dec. 1, 2022. [Online]. Available: https://mmwave.group.shef.ac.uk

[24] H. Wang, K. E. Kedze, and I. Park, "A high-gain and wideband series-fed angled printed dipole array antenna," *IEEE Trans. Antennas Propag.*, vol. 68, no. 7, pp. 5708–5713, Jul. 2020.

[25] U. Ullah, M. Al-Hasan, S. Koziel, and I. B. Mabrouk, "A series inclined slot-fed circularly polarized antenna for 5G 28 GHz applications," *IEEE Antennas Wireless Propag. Lett.*, vol. 20, pp. 351–355, 2021.

[26] S. Afoakwa and Y.-B. Jung, "Wideband microstrip comb-line linear array antenna using stubbed-element technique for high sidelobe suppression," *IEEE Trans. Antennas Propag.*, vol. 65, no. 10, pp. 5190–5199, Oct. 2017.

[27] C.-K. Hsieh, M. N. M. Kehn, and E. Rajo-Iglesias, "Design of a transverse slot array in groove gap waveguide using horns at 28 GHz band," in *Proc. IEEE Int. Symp. Antennas Propag. USNC-URSI Radio Sci. Meeting*, 2019, pp. 2045–2046.

[28] E. A. Ball, "Investigation into series-fed microstrip patch arrays at 26 GHz, 28 GHz and 48 GHz—Design, simulation and prototype tests," in *Proc. IEEE Texas Symp. Wireless Microw. Circuits Syst. (WMCS)*, 2021, pp. 1–6.

[29] H. Aliakbari, M. Mosalanejad, C. Soens, G. A. E. Vandenbosch, and B. K. Lau, "79 GHz multilayer series-fed patch antenna array with stacked micro-via loading," *IEEE Antennas Wireless Propag. Lett.*, vol. 21, pp. 1990–1994, 2022.

SUMIN DAVID JOSEPH received the B.Tech. degree (Hons.) in electronics and communication from CUSAT University, India, in 2012, the M.Tech. degree (Hons.) in communication systems from the Visvesvaraya National Institute of Technology, India, in 2015, and the dual Ph.D. degree (distinction) in electrical engineering from the University of Liverpool, U.K., and National Tsing Hua University, Taiwan.

He is currently working as a Postdoctoral Research Associate with The University of Sheffield. He was a Lab Engineer under CoE with the Visvesvaraya National Institute of Technology, India, from 2015 to 2017, where he was involved in projects of national importance. He has authored or coauthored more than 25 articles in peer-reviewed journals and conference proceedings. His research interests include self-biased circulators, mm-wave antenna arrays, rectifying antennas, MMIC circuits, RFIC, rectifiers, integrated circuit designs, flexible electronics, wireless power transfer, energy harvesting, and TMA antenna arrays. He is a Technical Reviewer for leading academic journals and conferences, including IEEE TRANSACTIONS OF ANTENNA AND PROPAGATION, IEEE ANTENNA AND WIRELESS PROPAGATION LETTERS, and IEEE ACCESS.

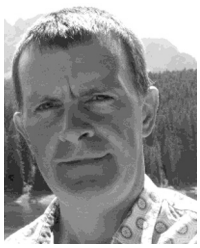

EDWARD A. BALL (Member, IEEE) was born in Blackpool, U.K., in November 1973. He received the Master of Engineering degree (Hons.) in electronic systems engineering from the University of York, York, U.K., in 1996.

After graduating, he worked in industry for 20 years, first spending 15 years working as an Engineer, a Senior RF Engineer, and finally a Principal RF Engineer with Cambridge Consultants Ltd., Cambridge, U.K. He then spent five years as a Principal RF Engineer and a Radio Systems Architect with Tunstall Healthcare Ltd., Whitley, U.K. In November 2015, he joined the Department of Electronic and Electrical Engineering, The University of Sheffield, Sheffield, U.K., where he is currently working as a Reader in RF Engineering and has a UKRI Future Leaders Fellowship. His research interests cover all areas of radio technology, from RF system design, RF circuit design (sub-GHz to mm-wave), and the application of radio technology to real-world industrial and commercial problems. He has a particular passion for RF hardware design. He is a member of the IET and a Chartered Engineer.